

# TPD study about the surface modification of some Ni/spinel catalysts in the hydrodechlorination of 1,2,4-trichlorobenzene. Influence on hydrogenation ability

Y. Cesteros<sup>a</sup>, P. Salagre<sup>a</sup>, F. Medina<sup>b</sup> and J.E. Sueiras<sup>b,\*</sup>

<sup>a</sup> *Facultat de Química, Universitat Rovira i Virgili, Pl. Imperial Tarraco, 1, 43005 Tarragona, Spain*

<sup>b</sup> *Escola Tècnica Superior d'Enginyeria, Universitat Rovira i Virgili, Pl. Imperial Tarraco, 1, 43005 Tarragona, Spain*  
E-mail: jsueiras@etse.urv.es

Received 15 December 1999; accepted 25 April 2000

NiAl<sub>2</sub>O<sub>4</sub> supports and fresh and reactivated Ni/NiAl<sub>2</sub>O<sub>4</sub> catalysts were tested in the gas phase hydrodechlorination of 1,2,4-trichlorobenzene. Fresh catalysts hydrogenate 1,2,4-trichlorobenzene to cyclohexane in the first 30 min of reaction at 523 K. An irreversible partial chlorination of the catalytic surface makes the hydrogenation of the aromatic ring difficult.

**Keywords:** cyclohexane, Ni/spinel, 1,2,4-trichlorobenzene, surface chlorination

## 1. Introduction

Chlorinated aromatic compounds are known to be highly toxic to the environment. Catalytic hydrodechlorination is one of the better ways of treating chlorinated organic substances to obtain compounds with lower or null toxicities [1–3].

This catalytic process has been studied with bulk and supported catalysts of Rh, Pd and Pt [4–7] and more recently with Ni catalysts [8–10]. Also, nickel/spinel catalysts are becoming increasingly interesting because this form of nickel supported on a high surface area spinel [11–14] is more resistant to deactivation by coke formation in steam reforming than when deposited on an inert support [11,12,14].

There are only a few references to obtaining cyclohexane from the hydrodechlorination of chloroaromatic compounds. The saturation of the final benzene ring may become difficult because of the resonance stabilization in aromatics. Another important factor is the action of the HCl produced during the hydrodechlorination reaction, which could irreversibly affect some active centres of the catalyst. Coq et al. [5] obtained low amounts of cyclohexane from the hydrodechlorination of chlorobenzene using Rh/Al<sub>2</sub>O<sub>3</sub> and Pd/Al<sub>2</sub>O<sub>3</sub> catalysts. On the other hand, Srinivas et al. [15] obtained high selectivities to cyclohexane for the same reaction using Pt/Al<sub>2</sub>O<sub>3</sub> catalysts modified with MgO. This modification increases the deactivation resistance of Pt catalysts in the hydrodechlorination of chlorobenzene.

We studied the hydrodechlorination of polychlorinated aromatic compounds on Ni/spinel catalysts [16]. These catalysts were highly resistant to the action of HCl, as it was reflected by the fact that there was only a slight decrease in

the activity before reaching the “plateau” (2 h). However, cyclohexane was not detected at “plateau”.

The aim of this work was the study of the surface modification of several high-area Ni/NiAl<sub>2</sub>O<sub>4</sub> catalysts due to the hydrodechlorination reaction in order to better understand how surface chlorination affects the hydrogenation of the aromatic ring. These results have been correlated with the yield of cyclohexane in the hydrodechlorination of 1,2,4-trichlorobenzene in the gas phase.

## 2. Experimental

Two nickel aluminate precursors were prepared following the coprecipitation method of nickel and aluminium nitrate solutions (Ni/Al = 1/2) described elsewhere [17]. These precursors were designated as D<sub>1</sub> (precipitated at 298 K) and D<sub>2</sub> (precipitated at 348 K). Two spinels were obtained by calcining D<sub>1</sub> and D<sub>2</sub> at 773 K for 5 h (referred to as Sp<sub>1</sub> and Sp<sub>2</sub>, respectively). The spinels were impregnated with aqueous solutions of Ni(NO<sub>3</sub>)<sub>2</sub>·6H<sub>2</sub>O to obtain a final composition of 0.21 g Ni/g NiAl<sub>2</sub>O<sub>4</sub> and then they were calcined at 523 K for 30 min (Sp<sub>1</sub>I and Sp<sub>2</sub>I). The reduction of the catalytic precursors (impregnated spinels) and supports (spinel) were carried out under pure H<sub>2</sub> at 673 K for 6 h (Sp<sub>1</sub>IR, Sp<sub>2</sub>IR, Sp<sub>1</sub>R, Sp<sub>2</sub>R). The supports were reduced to be characterized in order to see how the support affects the final structural properties of the catalysts.

Spinel supports and fresh catalysts (before the hydrodechlorination reaction), used catalysts and reactivated catalysts (after the hydrodechlorination reaction) were characterized by XRD, BET, SEM and TPD techniques. The catalysts were reactivated (after their use in the hydrodechlorination reaction) by H<sub>2</sub> treatment at 400 °C for 6 h.

\* To whom correspondence should be addressed.

Powder X-ray diffraction patterns (XRD) of the samples were obtained with a Siemens D5000 diffractometer using nickel-filtered Cu K $\alpha$  radiation. The patterns were recorded over a range of  $2\theta$  angles from  $10^\circ$  to  $90^\circ$  and the crystalline phases were identified using the files of the Joint Committee on Powder Diffraction Standards (JCPDS). The  $2\theta$  angles (with the relative intensities in parentheses), taken from the JCPDS files, are the following:  $37.01^\circ$  (100),  $45.00^\circ$  (65) and  $65.54^\circ$  (60) for the NiAl<sub>2</sub>O<sub>4</sub> phase,  $37.29^\circ$  (91),  $43.30^\circ$  (100) and  $62.91^\circ$  (57) for the NiO phase and  $44.51^\circ$  (100),  $51.85^\circ$  (42) and  $76.36^\circ$  (21) for the Ni phase. This technique was also used to determine the reduction degree ( $\alpha$ ) of the catalysts by the Rietveld method [18]. This method enables quantitative phase analysis of multicomponent mixtures to be performed from the X-ray powder diffraction data.

The BET surface areas were calculated from the nitrogen adsorption isotherms at 77 K using a Micromeritics ASAP 2000 surface analyser and a value of 0.164 nm<sup>2</sup> for the cross-section area of the nitrogen molecule.

Scanning electron micrographs were obtained with a Jeol JSM-35C scanning microscope operating at an accelerating voltage of 35 kV, a work distance (wd) of 16 mm and magnification values in the range 40000–50000 $\times$ .

Temperature-programmed desorptions (TPD) were obtained with a Fisons QTMD 150 gas desorption unit equipped with a 273–1273 K programmable-temperature furnace and a mass spectrometer detector.

Three experiments of TPD were performed as follows:

- First experiment: the catalytic precursors were reduced in the TPD burette under the same reduction conditions as those in which the catalysts were prepared for the catalytic system. The samples were then cooled at room temperature, evacuated at low pressures (<1 Pa) and the H<sub>2</sub> TPD of these fresh catalysts were obtained by heating at a rate of 10 K/min up to 800 K under vacuum.
- Second experiment: a new fresh catalyst was prepared and the hydrodechlorination reaction of 1,2,4-trichlorobenzene at 423 K (the lowest reaction temperature used in the catalytic study) was performed *in situ* in the TPD burette by passing a H<sub>2</sub>/1,2,4-trichlorobenzene flow during 2 h. Then, an Ar flow was passed through the used catalyst at 433 K for 1 h to remove the reversible adsorbed species on the catalyst surface. The temperature was then lowered and a H<sub>2</sub> flow was passed through the used catalyst. The H<sub>2</sub>, HCl and Cl<sub>2</sub> TPDs of the used catalysts were obtained in the same conditions as those described above for the H<sub>2</sub> TPD of fresh catalysts.
- Third experiment: the used catalysts of the second experiment were reactivated (by hydrogen treatment at 673 K for 6 h) and the H<sub>2</sub>, HCl and Cl<sub>2</sub> TPDs of the reactivated catalysts were also performed from room temperature by heating at a rate of 10 K/min up to 800 K under vacuum.

The gas phase hydrogenation of 1,2,4-trichlorobenzene was studied in a fixed-bed flow tubular reactor (1.1 cm internal diameter and 20 cm length) heated by an oven equipped with a temperature control system. The reactor was filled with catalyst (200 mg), previously ground and sieved at 0.2–0.7 mm. The catalytic reaction was tested at 1 atm pressure, with a reactant/H<sub>2</sub> molar ratio of 1/1500 and a space velocity of 60000 h<sup>-1</sup>. The reaction temperatures ranged between 523 and 423 K and the products were analyzed with an on-line gas chromatograph HP 5890 equipped with a packed column and a flame ionization detector.

The catalysts did not show external or internal diffusional limitations as the residence times lie on the linear portion of the curve obtained when plotting conversion against residence time for different catalyst volumes.

Conversions and selectivities were defined by the following equations: conversion (%) = (mol of 1,2,4-trichlorobenzene consumed)  $\times$  100/(mol of 1,2,4-trichlorobenzene charged); selectivity (%) = (mol of one product of reaction)  $\times$  100/(mol of 1,2,4-trichlorobenzene consumed). The conversion and selectivity values given in section 3 were measured in the first 30 min of reaction and at the “plateau” or stationary regime, after about 2 h run for the two catalysts. The carbon mass balance of the process was always held.

### 3. Results and discussion

The high-area NiAl<sub>2</sub>O<sub>4</sub> spinels and the Ni/NiAl<sub>2</sub>O<sub>4</sub> catalysts were characterized by XRD, BET and SEM techniques.

The reduced spinels Sp<sub>1</sub>R (180 m<sup>2</sup>/g) and Sp<sub>2</sub>R (125 m<sup>2</sup>/g) showed a NiAl<sub>2</sub>O<sub>4</sub> phase for both samples and an additional NiO phase for Sp<sub>2</sub>R. The catalysts, prepared from impregnation–calcination of the spinels, showed three phases: a NiO phase (in greater amount for sample Sp<sub>2</sub>IR), a NiAl<sub>2</sub>O<sub>4</sub> phase and a metallic Ni phase. The BET area was slightly higher for catalyst Sp<sub>1</sub>IR (99 m<sup>2</sup>/g) than Sp<sub>2</sub>IR (95 m<sup>2</sup>/g).

The micrographs of the impregnated–calcined spinels obtained by SEM allow to observe the similar morphology of the NiO particles for both samples. Figure 1 shows small octahedral particles of NiO of about 1000 Å for the catalytic precursor Sp<sub>2</sub>I. The HCl resistance has been related to the presence of large and well-defined particles [9,16].

#### 3.1. TPD studies

To obtain information about the kind and amount of adsorbed hydrogen available before and during the hydrodechlorination reaction, three TPD experiments of H<sub>2</sub> for the fresh catalyst, used catalyst and reactivated catalyst were performed on Sp<sub>1</sub>IR and Sp<sub>2</sub>IR samples in the conditions reported in section 2. Also, the hydrogen TPD of the reduced supports (spinel) were studied.

The mechanisms of adsorption–desorption of hydrogen can become extremely complex [19–38], especially over

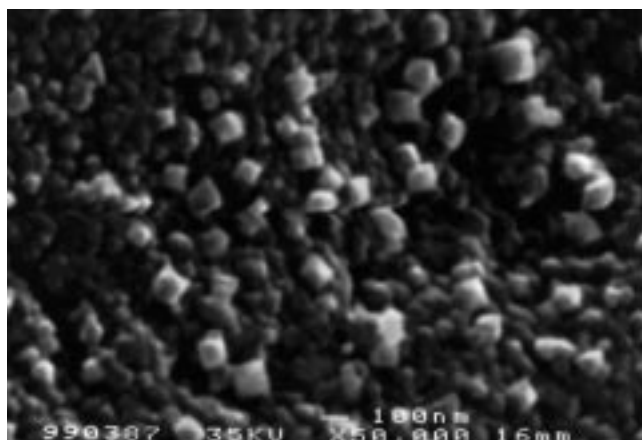


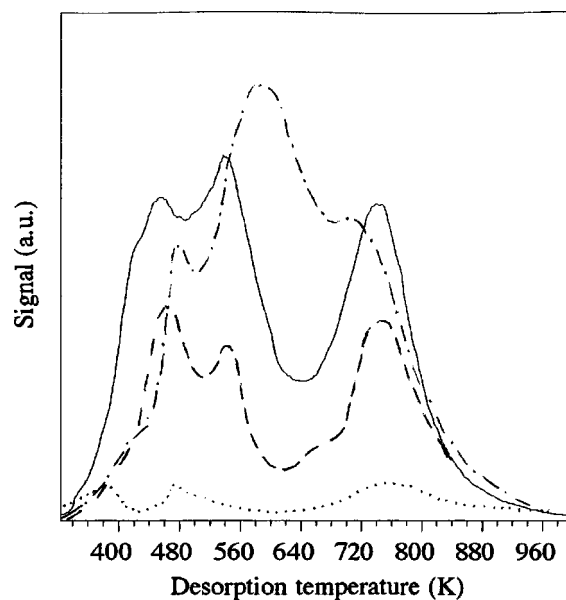
Figure 1. Scanning electron micrograph taken from the surface of the catalyst precursor  $\text{Sp}_2\text{I}$ :  $\text{NiO/NiAl}_2\text{O}_4$  (magnification  $\times 50000$ ).

supported catalysts, because phenomena related to the interaction between the active phase and the support can interfere. The number and approximate population of every adsorbed species depend on many factors: how the catalyst was prepared, the kind of support used and the experimental conditions of the measurement such as the weight of the sample examined, the flow rate of the carrier gas, the use of ultrahigh vacuum (UHV) or the shape of the reactor system which affect the removal conditions of desorbed hydrogen. Although there are many factors which influence the hydrogen TPDs obtained, the hydrogen desorption peaks with temperatures of desorption below 625 K have been related to the activity performance of different nickel catalysts [9,30,39].

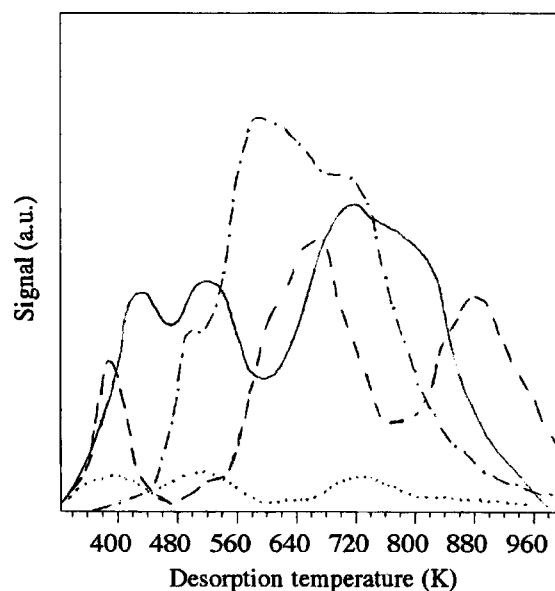
Figure 2 (a) and (b) shows the desorption peaks of hydrogen for the samples mentioned above. TPD plots for fresh catalysts had different types of adsorbed hydrogen, which may be related to their different active sites. Catalyst  $\text{Sp}_1\text{IR}$  has three desorption peaks whereas catalyst  $\text{Sp}_2\text{IR}$  has four (with lowest intensities). They show two desorption peaks in a low-temperature region below 625 K (with maxima at 440 and 540 K, respectively) and one or two desorption peaks (broader for catalyst  $\text{Sp}_2\text{IR}$ ) in a high-temperature region with maxima between 720–740 and 780 K.

The low desorption temperature region (below 625 K) has been related to different adsorption states of the hydrogen for other supported nickel catalysts [30]. Several authors have assigned the high-temperature peaks to the hydrogen spillover that takes place during high-temperature treatments of the catalysts (above 773 K) [19,31]. However, we cannot rule out assigning these peaks to other adsorption states of hydrogen on the metal surface (presumably related to a different morphology and size of the nickel particles), as observed for other nickel catalysts [8,9].

TPD plots for the corresponding reduced supports (figure 2 (a) and (b)) also showed low-temperature region peaks below 600 K (with maxima at 458 and 542 K for  $\text{Sp}_1\text{R}$  and 392 K for  $\text{Sp}_2\text{R}$ ) and high-temperature region peaks with maxima at 743 K for  $\text{Sp}_1\text{R}$  and 670 and 900 K for  $\text{Sp}_2\text{R}$ .



(a)



(b)

Figure 2.  $\text{H}_2$  TPD plots for the reduced support (---) and fresh (—), used (···) and reactivated (— · —) catalysts: (a)  $\text{Sp}_1\text{IR}$  and (b)  $\text{Sp}_2\text{IR}$ .

In all cases, the peaks with highest intensities are those of hydrogen desorbed in the high-temperature region.

We should note that the catalyst  $\text{Sp}_1\text{IR}$  (figure 2(a)) has the same kind of hydrogen adsorption sites but with different relative intensities than its reduced support. On the other hand, a quite different surface-site structure is shown by the hydrogen TPD of the catalyst  $\text{Sp}_2\text{IR}$  and its reduced spinel (figure 2(b)). In both cases, the intensities of the reduced spinels are lower than for impregnated samples, especially in the low-temperature region. This is in agreement with the small amount of metallic nickel phase of  $\text{Sp}_1\text{R}$  and  $\text{Sp}_2\text{R}$ , which is undetectable by XRD but confirmed by XPS studies [17].

The low hydrogen coverage  $\Theta_H$  after the hydrodechlorination reaction at 423 K observed for the used catalysts must be pointed out. This is caused by the formation of  $\text{NiCl}_2$  from the reaction of the metallic phase with the  $\text{HCl}$  produced during the reaction [5,8,9].

Comparison of the TPD curves for the fresh and reactivated catalysts  $\text{Sp}_1\text{IR}$  and  $\text{Sp}_2\text{IR}$  (figure 2 (a) and (b)) shows that an increase of the amount of hydrogen desorbed takes place. On the other hand, there is a clear loss of weakly adsorbed hydrogen and a shift of the desorption maxima to higher temperatures for the reactivated catalysts. The two reactivated catalysts show three hydrogen desorption peaks with similar maxima temperatures at 480–490, 590 and 710 K but with different relative intensities. The most intense peak desorbs hydrogen at 590 K.

During the hydrodechlorination reaction, there is a chemisorption of chlorine and the metallic nickel is transformed to small nickel chloride particles on the catalytic surface. After the reactivation of the catalyst, this nickel chloride formed on the surface is reduced again to metallic nickel under pure hydrogen. Assuming that the nickel chloride particles are smaller than those of metallic nickel, the new metallic nickel formed from the nickel chloride has a smaller particle size than the original metallic nickel obtained from the reduction of the nickel oxide on fresh catalysts. This could give place to an increase in the metallic area that might be responsible for the higher amount of hydrogen desorbed observed by TPD for the reactivated catalysts.

The  $\text{HCl}$  and  $\text{Cl}_2$  TPDs of used and reactivated catalysts were also performed in order to compare their abilities to eliminate the chlorine species formed during the reaction and to observe if a regeneration of the catalytic surface could take place. Despite the many works about hydrogen desorption on supported nickel catalysts reported [17,19–38], we have found *to our knowledge* no reference concerning  $\text{HCl}$  and  $\text{Cl}_2$  TPD studies on this kind of catalysts, so far.

Figure 3 (a) and (b) shows the  $\text{H}_2$ ,  $\text{HCl}$  and  $\text{Cl}_2$  TPDs for catalysts  $\text{Sp}_1\text{IR}$  and  $\text{Sp}_2\text{IR}$  respectively, after the hydrodechlorination reaction at 423 K. The two catalysts show three desorption peaks of hydrogen chloride and one desorption peak of chlorine (with different relative intensities). The maxima of hydrogen chloride desorption are 410, 538 and 1000 K for catalyst  $\text{Sp}_1\text{IR}$  and 440, 557 and 1200 K for catalyst  $\text{Sp}_2\text{IR}$ . The chlorine desorbs at temperatures below 625 K with one maximum at 420 and 438 K for catalyst  $\text{Sp}_1\text{IR}$  and  $\text{Sp}_2\text{IR}$ , respectively.

The hydrogen chloride is mainly generated by the desorption of hydrogen and chlorine strongly chemisorbed. The fact that the hydrogen chloride mainly desorbs at higher temperatures than the chlorine could be explained taking into account the thermodynamics of the reactions involved. The bonding energies at 298 K for the  $\text{H}_2$ ,  $\text{HCl}$  and  $\text{Cl}_2$  molecules are 436.0, 431.8 and 242.6  $\text{kJ mol}^{-1}$ , respectively. When the temperature of desorption is higher, the forma-

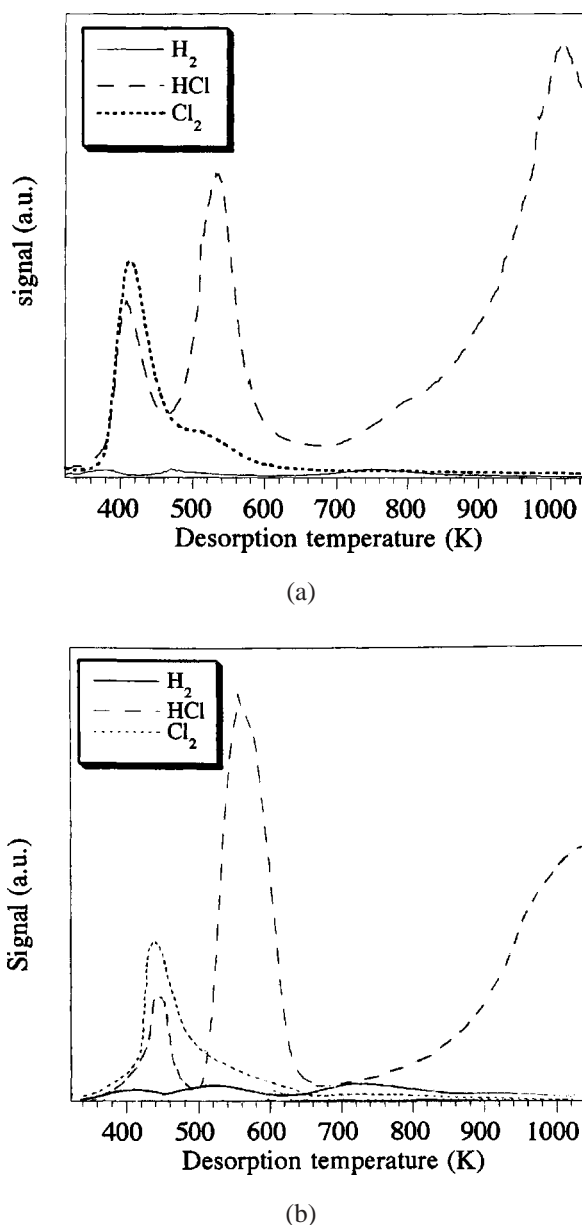


Figure 3.  $\text{H}_2$ ,  $\text{HCl}$  and  $\text{Cl}_2$  TPD plots for used catalysts: (a)  $\text{Sp}_1\text{IR}$  and (b)  $\text{Sp}_2\text{IR}$ .

tion of  $\text{Cl-Cl}$  is thermodynamically much less favourable compared to the other two possible bonds.

As observed, the total amount of hydrogen chloride and chlorine desorbed is much higher than the amount of hydrogen desorbed for the two used catalysts. This clearly indicates the high poisoning suffered by the catalyst at this low reaction temperature. The following step studied determines whether this chlorinated surface can be recovered after the catalysts are reactivated.

Figure 4(a) and (b) shows the  $\text{H}_2$ ,  $\text{HCl}$  and  $\text{Cl}_2$  TPDs for the catalyst  $\text{Sp}_1\text{IR}$  and  $\text{Sp}_2\text{IR}$ , respectively, after reactivating for 6 h under pure hydrogen. We can see that the desorbed chlorine and hydrogen chloride almost disappear between 325 and 750 K, although the most strongly chemisorbed hydrogen chloride remains.



Some studies correlate the binding strength of the chemisorbed hydrogen with the activity for a specific reaction. There is a quantitative correlation between the weakly

bound hydrogen (temperatures of hydrogen desorption between 323 and 500 K) and the specific activity of supported nickel catalysts for benzene, toluene and 1,2,4-trichlorobenzene hydrogenations [9,30,39].

Figure 2(a) shows that the fresh catalyst Sp<sub>1</sub>IR has the highest amount of weakly bound hydrogen and a high performance of this catalyst is expected both to hydrodechlorinate the halobenzene and hydrogenate the less reactive aromatic ring. Likewise, the used catalysts lose a similar amount of weakly and strongly adsorbed hydrogen (figure 3 (a) and (b)), which account for a decrease in the activity of both catalysts. By comparing with the fresh catalysts (figure 2), the hydrogen TPD curves obtained after reactivating the catalysts show a less recovering of the weakly adsorbed hydrogen but higher total amount of hydrogen. It seems clear that this fact should affect the activity and selectivity of the hydrodechlorination reaction.

### 3.2. Influence on hydrogenation ability

Table 1 summarises the conversions and product distributions for the hydrodechlorination reaction of 1,2,4-trichlorobenzene on Sp<sub>1</sub>IR and Sp<sub>2</sub>IR catalysts under the conditions described in section 2.

The fresh catalysts Sp<sub>1</sub>IR and Sp<sub>2</sub>IR were able to hydrogenate the 1,2,4-trichlorobenzene to cyclohexane in the first 30 min of the reaction at 523 K (at lower temperature there is not enough activation energy and at higher temperature molecules of low molecular weight are obtained), but when reaction time increases, the cyclohexane disappears and the main product is benzene “at plateau” (2 h). The catalyst which was the most active and selective towards benzene at all temperatures was Sp<sub>1</sub>IR with a conversion of 82% and a selectivity towards benzene of 87% at 523 K.

No cyclohexane was detected when the reduced spinels were tested in the hydrodechlorination reaction. Both the conversions and selectivities towards benzene were low, probably because less hydrogen was available as a result of the small amount of surface Ni.

Table 2 shows the conversions and product distributions for the hydrodechlorination reaction of 1,2,4-trichloro-

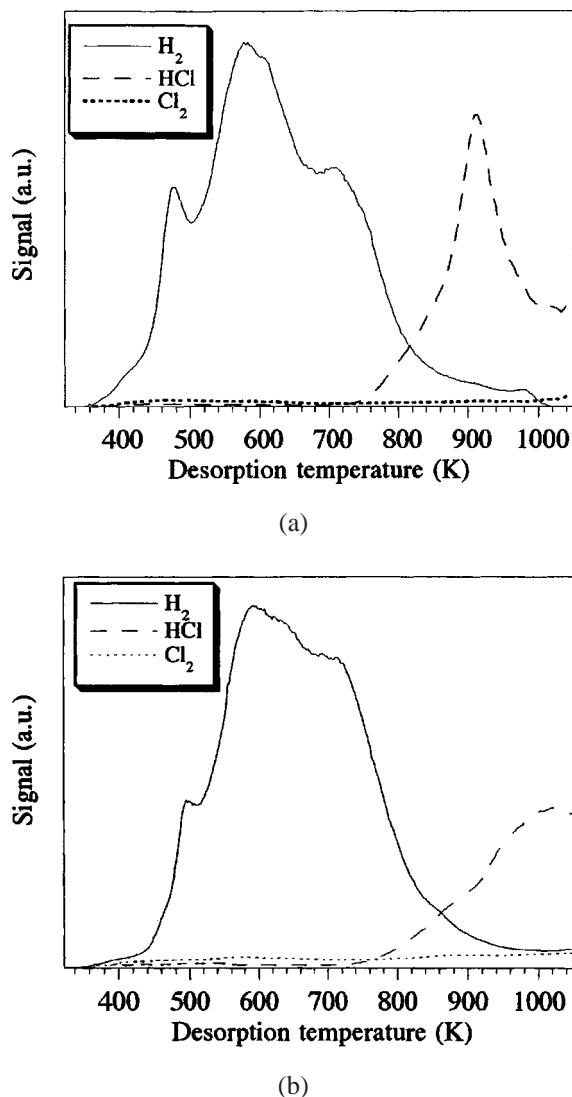


Figure 4. H<sub>2</sub>, HCl and Cl<sub>2</sub> TPD plots for reactivated catalysts: (a) Sp<sub>1</sub>IR and (b) Sp<sub>2</sub>IR.

Table 1  
Catalytic activities for the hydrodechlorination of 1,2,4-trichlorobenzene on fresh catalysts.<sup>a</sup>

T (K)	Sp <sub>1</sub> IR						Sp <sub>2</sub> IR					
	C (%)	Selectivity <sup>b</sup> (%)					C (%)	Selectivity <sup>b</sup> (%)				
		Chex	Bz	CBz	<i>o</i> -Cl <sub>2</sub> Bz	<i>p</i> -Cl <sub>2</sub> Bz		Chex	Bz	CBz	<i>o</i> -Cl <sub>2</sub> Bz	<i>p</i> -Cl <sub>2</sub> Bz
523 <sup>c</sup>	87	71	18	2	8	1	72	52	12	1	26	9
523 <sup>d</sup>	82	0	87	0	10	3	67	0	58	1	30	11
498	60	0	56	2	35	7	42	0	31	1	50	18
473	36	0	28	1	57	14	28	0	20	2	59	19
448	22	0	16	2	67	15	17	0	9	2	70	19
423	10	0	6	0	78	16	9	0	4	0	78	18

<sup>a</sup> T (K) – reaction temperature, C (%) – conversion.

<sup>b</sup> Chex – cyclohexane, Bz – benzene, ClBz – chlorobenzene, *o*-Cl<sub>2</sub>Bz – 1,2-dichlorobenzene, *p*-Cl<sub>2</sub>Bz – 1,4-dichlorobenzene.

<sup>c</sup> Values after 30 min of reaction.

<sup>d</sup> Values in the “plateau” (2 h).

Table 2  
Catalytic activities for the hydrodechlorination of 1,2,4-trichlorobenzene on reactivated catalysts.<sup>a</sup>

T (K)	Sp <sub>1</sub> IR						Sp <sub>2</sub> IR					
	C (%)	Selectivity <sup>b</sup> (%)					C (%)	Selectivity <sup>b</sup> (%)				
		Chex	Bz	CBz	<i>o</i> -Cl <sub>2</sub> Bz	<i>p</i> -Cl <sub>2</sub> Bz		Chex	Bz	CBz	<i>o</i> -Cl <sub>2</sub> Bz	<i>p</i> -Cl <sub>2</sub> Bz
523 <sup>c</sup>	100	0	64	36	0	0	85	0	49	20	24	7
523 <sup>d</sup>	96	0	60	30	8	2	79	0	46	16	30	8
473	67	0	13	14	46	27	51	0	11	9	60	20
423	25	0	2	2	74	22	22	0	2	1	78	19

<sup>a</sup> T (K) – reaction temperature, C (%) – conversion.

<sup>b</sup> Chex – cyclohexane, Bz – benzene, ClBz – chlorobenzene, *o*-Cl<sub>2</sub>Bz – 1,2-dichlorobenzene, *p*-Cl<sub>2</sub>Bz – 1,4-dichlorobenzene.

<sup>c</sup> Values after 30 min of reaction.

<sup>d</sup> Values in the “plateau” (2 h).

benzene on reactivated Sp<sub>1</sub>IR and Sp<sub>2</sub>IR catalysts. The main finding is that, in contrast to the fresh catalysts, no cyclohexane was detected in the first 30 min of reaction. Also, the reactivated catalysts are more active than the fresh catalysts but less selective towards benzene, and there is a considerable increase of chlorobenzene as a product of the reaction.

As commented above in the TPD studies, the formation of smaller metallic nickel particles, from the reduction of the nickel chloride originated on the surface during the hydrodechlorination reaction, could give place to an increase in the metallic area that may be responsible for the higher conversion values found for the reactivated catalysts (table 2). The hydrogen atmosphere in the reactivation process allows a more effective regeneration of the active phase than in the atmosphere of the hydrodechlorination reaction but the removal of the chlorine from the catalyst surface is not completed and the result is a catalyst with smaller metallic particles residuary chlorinated. This fact leads to a different surface-site structure.

The new surface has different hydrogen adsorption sites with a clear decrease in the hydrogen available on the surface at the reaction temperature used (confirmed by TPD). The main consequence is the loss in the ability to hydrogenate the aromatic ring, which confirms that breaking the C–Cl bond is easier than hydrogenating the benzene ring. The loss of weakly adsorbed hydrogen explains the lower selectivity to benzene and the higher selectivity to chlorobenzene observed for the reactivated catalysts (table 2) since the hydrodechlorination of 1,2,4-trichlorobenzene evolves with more difficulty to the total substitution of the chlorine atoms by hydrogen atoms.

#### 4. Conclusions

The high availability of hydrogen exhibited by the fresh catalysts (H<sub>2</sub> TPDs), under the reaction conditions used, explains their initial ability to hydrodechlorinate and hydrogenate the aromatic ring simultaneously. The rapid chlorination of the catalytic surface during the hydrodechlorination of 1,2,4-trichlorobenzene considerably decreases the hydrogen available in the reaction conditions and conse-

quently the cyclohexane disappears after 30 min of reaction. The most active and selective catalyst towards benzene is Sp<sub>1</sub>IR at all temperatures. The hydrogen TPDs for reactivated catalysts showed a higher amount of hydrogen desorbed but mainly at higher desorption temperatures than fresh catalysts. Therefore, reactivating the used catalysts allows the chlorine and hydrogen chloride to be removed from the catalyst surface but greatly reduces the weakly adsorbed hydrogen available at the reaction temperatures and, consequently, the ability to hydrogenate the aromatic ring.

#### References

- [1] B.F. Hagh and D.T. Allen, *Chem. Eng. Sci.* 45 (1990) 2695.
- [2] H.M. Freeman and R.A. Olexsey, *J. Air Pollut. Control. Assoc.* 36 (1986) 67.
- [3] B.F. Hagh and D.T. Allen, in: *Innovative Hazardous Waste Treatment Technology*, Vol. 1, ed. H.M. Freeman (Technomic, Lancaster, PA, 1990).
- [4] B. Coq, A. Tijani, R. Dutartre and F. Figueras, *J. Mol. Catal.* 79 (1993) 253.
- [5] B. Coq, G. Ferrat and F. Figueras, *J. Catal.* 101 (1986) 434.
- [6] A. Gampine and D.P. Eymann, *J. Catal.* 179 (1998) 315.
- [7] N. Balko, E. Prybylski and F. von Trentini, *Appl. Catal. B* 2 (1993) 21.
- [8] J. Estelle, J. Ruz, Y. Cesteros, R. Fernandez, P. Salagre, F. Medina and J.E. Sueiras, *J. Chem. Soc. Faraday Trans.* 92 (1996) 2811.
- [9] Y. Cesteros, P. Salagre, F. Medina and J.E. Sueiras, *Appl. Catal. B* 22 (1999) 135.
- [10] G. Tavoularis and M.A. Keane, *J. Mol. Catal. A* 142 (1999) 187.
- [11] A. Al-Ubaid and E.E. Wolf, *Appl. Catal.* 40 (1988) 73.
- [12] I.A.P.S. Murthy and C.S. Swamy, *J. Mater. Sci.* 28 (1993) 1194.
- [13] J.A. Peña, J. Herguido, C. Guimon, A. Monzon and J. Santamaria, *J. Catal.* 159 (1996) 313.
- [14] A. Bhattacharyya and V.W. Chang, in: *Catalysis Deactivation*, Stud. Surf. Sci. Catal., Vol. 88, eds. B. Delmon and G.F. Froment (Elsevier, Amsterdam, 1994).
- [15] S.T. Srinivas, P.S. Sai Prasad, S.S. Madhavendra and P. Kanta Rao, in: *Recent Advances in Basic and Applied Aspects of Industrial Catalysis*, Stud. Surf. Sci. Catal., Vol. 113, eds. T.S.R. Prasada Rao and G. Murali Dhar (Elsevier, Amsterdam, 1998) p. 835.
- [16] Y. Cesteros, P. Salagre, F. Medina and J.E. Sueiras, *Appl. Catal. B* 25 (2000) 213.
- [17] Y. Cesteros, P. Salagre, F. Medina and J.E. Sueiras, *Chem. Mater.* 12 (2000) 331.
- [18] D.L. Bish and S.A. Howard, *J. Appl. Cryst.* 21 (1988) 86.
- [19] Z. Pál and P.G. Menon, *Catal. Rev. Sci. Eng.* 25 (1983) 229.

- [20] Z. Paál and P.G. Menon, eds., *Hydrogen Effects in Catalysis* (Dekker, New York, 1988).
- [21] J.L. Falconer and J.A. Schwarz, *Catal. Rev. Sci. Eng.* 25 (1983) 141.
- [22] G.B. Raupp and J.A. Dumesic, *J. Catal.* 95 (1985) 587.
- [23] G.B. Raupp and J.A. Dumesic, *J. Catal.* 97 (1986) 85.
- [24] M. Arai, Y. Nishiyama, T. Masuda and K. Hashimoto, *Appl. Surf. Sci.* 89 (1995) 11.
- [25] P. Ferreira-Aparicio, A. Guerrero-Ruiz and I. Rodriguez-Ramos, *J. Chem. Soc. Faraday Trans.* 93 (1997) 3563.
- [26] N.M. Popova, L.V. Babenkova and D.V. Sokol'skii, *Kinet. Katal.* 10 (1969) 1177.
- [27] C.H. Bartholomew, *Catal. Lett.* 7 (1990) 27.
- [28] P.I. Lee and J.A. Schwartz, *J. Catal.* 73 (1982) 272.
- [29] J. Zielinski, *Polish J. Chem.* 69 (1995) 1187.
- [30] S. Smeds, T. Salmi, L.P. Lindfors and O. Krause, *Appl. Catal. A* 144 (1996) 177.
- [31] P. Kramer and M. Andre, *J. Catal.* 58 (1979) 287.
- [32] J.A. Konvalinka, P.H. van Oeffelt and J.J.F. Cholten, *Appl. Catal.* 1 (1981) 141.
- [33] G.D. Weatherbee and C.H. Bartholomew, *J. Catal.* 87 (1984) 55.
- [34] R. Spinicci and A. Tofanari, *React. Kinet. Catal. Lett.* 27 (1985) 65.
- [35] Y. Ikushima, M. Arai and Y. Nishiyama, *Appl. Catal.* 11 (1984) 305.
- [36] P.G. Glugla, K.M. Bailey and J.L. Falconer, *J. Catal.* 115 (1989) 24.
- [37] J.L. Rankin and C.H. Bartholomew, *J. Catal.* 100 (1986) 533.
- [38] D.M. Stockwell, A. Bertucco, G.W. Coulston and C.O. Bennet, *J. Catal.* 113 (1988) 317.
- [39] P. Marécot, E. Paraiso, J.M. Dumas and J. Barbier, *Appl. Catal.* 74 (1991) 261.